

---

## **MINERALOGY AND GEOCHEMISTRY OF STREAM SEDIMENTS OF SOUTHEAST WADI GHADIR, SOUTH EASTERN DESERT, EGYPT**

---

**MAHMOUD, M.A.M, KAMAR, M.S. AND HUSSEIN, K.H.**

*Nuclear Materials Authority P.O. Box 530 Maadi-Kattamya-Cairo-Egypt*

---

### **ABSTRACT**

*Southeast Wadi Ghadir area is located between latitudes 24° 47' 00" and 24° 49' 00" and longitudes 34° 58' 18" and 34° 59' 30". Geological and geochemical studies were carried out on the stream sediments and adjacent granites along some tributaries of Southeast Wadi Ghadir area, Southeastern Desert, Egypt. This investigation was carried out in order to identify the rock units with their stream sediments and to determine the concentration and distribution of trace elements granites with a view to elucidate the mineral potentials of the studied area.*

*Geological studies reveal the two rock types of granites, which are granodiorites and syenogranites. Granodiorites are composed of plagioclase, quartz, K-feldspar as essential felsic minerals. Biotite and hornblende are the essential mafic minerals. Apatite, zircon and opaques are accessory minerals. Syenogranites are composed of K-feldspar, quartz, plagioclase, biotite, as essential mineral constituents, while muscovite, zircon, allanite, apatite and opaques are accessories.*

*The analytical results reveal that the trace elements analyzed for granitoid rocks and stream sediments include; Cr, Ni, Cu, Zn, Zr, Rb, Y, Ba, Pb, Sr, Ga, V and Nb, which reveal that the stream sediments show higher average contents of most of the trace elements than the adjacent granitoid rocks except Ga which is not detected in the analyzed stream sediments samples.*

*Mineralogically, some important minerals were recorded in this study as; monazite, pseudo-autunite, goethite, hematite, pyrite, cinnabar, wulfenite, galena, natro-jarosite, titanite, and anatase.*

*Radiometrically, the syenogranites had eU more than twice Clark value; this indicates that the syenogranites were uraniumiferous and have been subjected to post-magmatic changes. Radiometric investigation of the studied stream sediments samples showed that the eU ranged from 5.0 ppm to 19 ppm and eTh ranges from 11 ppm to 92 ppm at the surface, while with depth the eU ranges from 6.0 ppm to 45.6 ppm and eTh ranges from 10 ppm to 52 ppm. The radioactivity increases with depth in all studied samples except sample number 2, indicating that uranium add to stream sediments from the adjacent granitic rocks.*

*Keywords: Mineralogy, Geochemistry, Wadi Ghadir, Stream sediments, Syenogranites, Radiometry.*

### **INTRODUCTION**

Hume (1935), was the first to classify the Egyptian basement rocks, he established four-fold subdivisions; starting with the oldest: 1-Proterarchean, 2- Metarchean, 3- Eparchean, and 4-late Precambrian or Gattarian. The oldest rocks in Hume's classification were the fundamental gneisses (granitic gneisses) that occur at Migif - Hafafit area. Similar outcrops occurring at Wadis; Nugrus, Sikait, Abu Rushied areas (Basta, and Zaki, 1961; El Shazly and Hassan, 1972; Saleh 1997) and at Gabel El Sibai area (Sabet, 1961; Ali, 2001 & 2013), at Gabel Meatiq area (El Gaby, 1975; Habib et al., 1982; El Nady, 1982), Abu Swayel area ( El Shazly et. al., 1973), Wadi Ghadir ( El Maghraby, 1987; Takla et al., 1992; El Bayoumi 1980), and in Sinai at Wadi Feiran ( Schurmann,1966; El Gaby and Ahmed, 1980; Shimron, 1980).

The Eastern Desert of Egypt represents the Western part of the Arabian-Nubian Shield, which characterized by the widespread occur-

rence of granitic rocks. Continuous granite series was suggested by El Gaby (1975) as two granite groups; this was refined later by (El Gaby and Ahmed, 1980; El Gaby and Habib, 1982) into a syn-to post orogenic calc-alkaline series and a post-orogenic alkaline to per-alkaline series. Hussein et al. (1982), proposed a new classification for the Egyptian granites, which classified into three groups namely GI, GII, and GIII granites. The rocks occur between Wadi Ghadir and Wadi El Gemal includes fall into three domains;

i-The gneisses, migmatites, and amphibolites domain.

ii-The ophiolitic mélange domain.

iii-The intrusive domain.

Sabet et al. (1978) and El Bayoumi (1980) classified the rocks that crop out along the eastern part of Wadi Ghadir as granites, belonging to the older and younger (Gattarian) granites. Ibrahim and Ali (2003) studied the two mica granites (syenogranite) showing shear zone striking

NE-SW cutting the two mica granite, rich in visible uranophane mineral filling fracture. Ali and Lentz (2011) studied the mineralogy, geochemistry and age dating of the shear zone-hosted Nb-Ta, Zr-Hf, Th, U-bearing granitic rocks in the Ghadir and El-Sella areas, southeastern desert, Egypt. Raslan and El-Feky (2012) studied the same shear zone and revealed the presence of uraninite, uranophane, thorite, Ce-monazite and zircon. The present work focusing on the stream sediments close to the shear zone concerning the study of geology, geochemistry and mineral concentrates in the stream sediments and adjacent granites.

### **WADI GHADIR BASIN**

Wadi Ghadir is a seventh order fan shaped basin (Fig. 1); with asymmetrical shape. The main channel of Wadi Ghadir flows NW-SE at its upper part, and E-W at its lower part towards the Red Sea. The basin mouth is crossed by a short segment of the Red Sea coastal road, which is strongly vulnerable to flooding (Ahmed, 2001 and Mahmoud, 2005).

### **GEOLOGIC SETTING**

The studied area is a part from Wadi Ghadir, lies near the downstream of the Wadi to the south of Marsa Alam coastal City. This area was mapped by Takla et al. (1987a and 1992), they interpreted its geologic history as consist of the following events from oldest to youngest: 1) old metamorphic rocks, composed of biotite granodiorite gneisses, migmatitic granite gneisses, granite mobilizates and amphibolite enclaves, 2) Ophiolitic mélange, and 3) Intrusive granitoids, composed of diorites, granodiorites and granites. They considered that the occurred old metamorphic rocks represent a small window of an old continental crust, representing Pre-Pan-African rocks.

The studied area (Fig. 2) is characterized by low-to moderate-relief and consists of older and younger granitoid rocks. These rocks are classified into oldest granodiorites and youngest syenogranites.

The studied granodiorites, which exposed in the east and west parts of the studied area (Fig.2), show low-to moderate relief terrains and exhibit

sharp contact with the younger granites (Fig. 3). The granodiorite rocks show medium to coarse-grained, grayish in colour, Joints, fractures and faults are frequently dissected the pluton.

The younger granites of the studied area are represented by syenogranites, exposed to the north and middle parts of the map (Fig. 2) The rock is medium- to coarse-grained, pink in colour and forming medium to high relief mountain terrains. They show cavernous and exfoliation weathering, highly jointed and fractured. Some fractures exhibit high alteration products represented by hematitization, and recorded high radioactivity (Ibrahim and Ali, 2003).

### **PETROGRAPHY**

The studied granodiorite rocks are composed of plagioclase, quartz, K-feldspar as essential felsic mineral constitutes, in addition biotite and hornblende are the essential mafic mineral constitutes. Apatite, zircon and opaques are the accessory minerals. Plagioclase (An20-40) forms euhedral to subhedral crystals showing various dimensions. Plagioclase megacrysts may poikilolithically host fine crystal of biotite, hornblende and quartz. Partial alteration of plagioclase to saussurite and muscovite is observed (Fig. 4). Quartz occurs as subhedral to anhedral crystals and filling the interstitial spaces between other minerals but in few cases quartz crystals show undulose extinction and granulated boundaries (Fig. 4). K-feldspar exhibits subhedral to anhedral crystals ranging in size and represented by orthoclase and microcline microperthite and partial alteration to kaolinite are observed (Fig. 4). Biotite is the dominant mafic mineral occurs as euhedral to subhedral crystals associated with zircon, apatite, opaque and quartz (Fig. 4). Alteration of biotite to chlorite and opaque is observed and usually starts along the cleavage plane. Hornblende occurs as euhedral to subhedral elongated crystals, it poikilolithically encloses quartz, titanite and apatite. It is partly altered to chlorite and opaque. Apatite exists as long prismatic crystals associated with biotite and hornblende. Zircon forms euhedral to subhedral crystals showed pleochroic haloes due to radiogenic effects (Fig. 5).

[The microscopic studies of the syenogranite rocks show essentially composed of K-feldspar, quartz, plagioclase, biotite, while muscovite, zircon, allanite, apatite and opaques are accessories. The K-feldspars occur as subhedral to anhedral crystals and is represented by orthoclase micropertite and microcline micropertite, sometimes altered to kaolinite and poikilitically encloses quartz and opaques. Quartz occurs as subhedral to anhedral crystals and interstitial grains exhibiting undulose extinction. The plagioclase (An9-15) occurs as euhedral to subhedral crystals. It exhibits simple twinning and show partial saussuritization. Biotite occurs as euhedral to subhedral elongate to flakey crystals corroded by quartz and micropertite and shows fairly alteration to chlorite (Fig.6). Muscovite occurs in accessory amount as euhedral to subhedral colourless flakes. Zircon occurs as euhedral to subhedral prismatic crystals. It attains pleochroic haloes due to radiogenic effects and associated with biotite. Apatite exhibits as euhedral prismatic crystals in association with biotite, allanite and plagioclase (Fig. 6). Allanite occurs as euhedral yellowish brown crystals associated with plagioclase and biotite (Fig. 7). Opaques form as subhedral to anhedral crystals usually associated with mafic constituents.

#### **METHODOLOGY**

Twenty representative samples were collected from the studied area; five samples from the granodiorites, five samples from the syenogranites and ten stream sediments samples. The collected samples are located on the geologic map of the studied area (Fig. 2). The trace elements were determined by the XRF technique in the Nuclear Materials Authority (NMA) laboratories and the obtained data are given in table (1).

Sampling was carried out on pits at depth (Fig. 8) is varying from 30 to 50 cm after eliminating the windblown sand, which predominant in the mid-fractions. The sediments were sieved to minus 1mm in the field, where each sample was measured radiometrically by RS-230 instrument two times; the first before taking the sample (surface) and the second after taking the sample. Each sample varies in weight from 5-6 kg., after quartering step.

#### **GEOCHEMISTRY**

While the analytical results for the trace elements geochemistry are presented in table (1). The selected trace elements analyzed include; Cr, Ni, Cu, Zn, Zr, Rb, Y, Ba, Pb, Sr, Ga, V, and Nb, as in table (1).

The results of trace elements analysis of the studied samples, the statistical summary of the distributed trace elements concentration in the study area are represented in table (1) and the histogram (Fig. 9). From the obtained data syenogranites show high average contents for most of the analyzed trace elements than in the granodiorite rocks except Nb, Ba, Pb and Sr on the other hand. Stream sediments have relatively high average values in the most of the trace elements compared to the granodiorites and syenogranites except Zr, Rb, Y, Ba, Sr and Nb, While Ga was not detected in the stream sediments.

All other trace elements like Zr, Rb, Y, Ba, Sr and Nb, are observed to be lower than their respective background value, so it can be inferred that such elements are depleted in the studied area. It can be observed from the correlation matrix between the almost trace elements of the studied stream sediments that a very strong correlation exist between them (Table 2). The very strong correlation indicating that the trace element constituents are governed by the same geochemical factors and are from the same source.

#### **MINERALOGY**

After sieving the collected samples in the field with minus 1mm (-1mm), they are washed by seawater until it became clear leaving only the heavy concentrates. Starting with one kilogram (1kg) weight sample (Table 2) to be sieved into three parts; > 0.5mm, 0.50-0.125mm and < 0.125mm, and weighting for further treatments. Hassaan (1974) and Hassan and Al-Hawary (1989) recommended that the minus 0.5mm (-0.5mm) size fraction as the most and best suitable size fraction containing the highest anomalous content of metals in Egypt like (Cu-Mo, Pb-Zn, Au, W and Sn). In this study the 0.5-0.125mm fraction size is recommended.

The fraction (0.5-0.125mm) was subjected to heavy minerals separation using the bromoform

liquid (sp.gr.=2.85gm/cm<sup>3</sup>) to separate the heavy mineral fraction from the light mineral fractions. The obtained data and the attached histogram are listed in table (4).

Table (4) with the attached histogram shows that the highest heavy mineral concentrates are represented in sample no.9, while sample no.6 showing the lowest heavy mineral concentrates.

The heavy fractions were subjected to magnetic separation by using a Frantz isodynamic separator, which separate the heavy fraction into; magnetic and nonmagnetic minerals. The nonmagnetic minerals fractions are identified by using X-ray diffraction (XRD). The following minerals were identified as; monazite, lepidocrocite, wulfenite, cinnabar, pyrite, galena, goethite, hematite, jarosite, natrolite, natro-jarosite, titanite, anatase and tychite, listed in table (5).

Figure (10) illustrates the percentage of non-magnetic minerals at different studied stream sediments samples, where: In sample No.1, monazite is the dominant mineral represents 50% of the sample by volume, then goethite and hematite equal to 40% and the lowermost mineral is lepidocrocite represent 10%. In sample No.2, goethite, natrolite and jarosite are the dominant minerals represent 50% of the sample by volume, and then monazite equal to 40% and the lowermost mineral is galena represent 10%. In sample No.3, goethite, natrolite and jarosite are the dominant minerals represent 60% of the sample by volume, then monazite equal to 40%. In sample No.4, titanite, natro-jarosite, jarosite and anatase are the dominant minerals represent 60% of the sample by volume, then goethite equal to 30% and the lowermost mineral is lepidocrocite represent 10%. In sample No.5, goethite and hematite are the dominant minerals represent 90% of the sample by volume, and then lepidocrocite is the lowermost mineral represents 10%.

In sample No.6, monazite is the dominant mineral represents 70% of the sample by volume, then goethite, hematite and tychite equal to 30%. In sample No.7, goethite and hematite are the dominant minerals represent 60% of the sample by volume, whereas monazite equals 40% by volum. In sample No.8, monazite is the dominant mineral represents 60% of the sample

by volume, and then goethite, hematite and pyrite equal to 30% and tychite is the lowermost mineral represents 10%. In sample No.9, titanite, natro-jarosite, anatase and tychite are the dominant minerals represent 50% of the sample by volume and then goethite and hematite represents 40%, cinnabar mineral is the lowermost and represents 10%. In sample No.10, goethite, tychite and wulfenite are the dominant minerals represent 80% of the sample by volume, and then titanite, natro-jarosite and anatase represent 20%.

The following results are the short notes about the identified minerals in the studied stream sediment samples, which they are confirmed by the XRD technique and seen by the binocular microscope.

1-Monazite [(LREE, Th) PO<sub>4</sub>] occurs as brown to reddish brown prismatic crystals or even tabular habit (Figs. 11A, 12 and 13) from samples No. 1, 2, 3, 6, 7 and 8. Monazite have a wide range of LREE, it is iso-structural with Cheralite (RE, Th, Ca, U) (P,Si)O<sub>4</sub> and Huttonite (ThSiO<sub>4</sub>), which they have highly ceric REE distributions (Bowles et al., 1980; Pabst and Hutton, 1951). Thorium is usually exists in monazite in substitution for the REE. Jensen (1976) concluded that the monazite structure would accept REE ions with ionic radii between those of La and Eu.

2- Lepidocrocite (FeO(OH)•H<sub>2</sub>O) is yellowish brown in colour (Figs. 11B and 14). It is exist in the samples No.1, 4 and 5.

3- Goethite FeO (OH) is reddish and brownish black in colour (Figs. 11C, 14, 18, 19 and 22) and formed due to the disintegration of pyrite (FeS<sub>2</sub>). It is exist in the all studied samples.

4-Hematite (Fe<sub>2</sub>O<sub>3</sub>) exists in the samples No.1, 5, 6, 7, 8 and 9 as granular grains with reddish brown to black in colour (Figs. 11D, 15 and 16). Hematite is hexagonal system and not susceptible to magnetization.

5-Pyrite (FeS<sub>2</sub>) occurs in the sample No.8, as cubes, octahedral or combination from these forms (Figs. 11E & 16). It is crystallized in cubic system and shows brownish colour with metallic luster.

6-Cinnabar (HgS) exists in the sample No.9 reflects orange to red in colour (Figs. 11F and 17). Cinnabar is a highly toxic, naturally occurring form of mercury mineral, which was used in the ancient past for producing a bright orange (vermillion) pigment on ceramics, murals, tattoos, and in religious ceremonies.

7-Wulfenite (PbMoO<sub>4</sub>) was recorded in the sample No. 10 (Fig. 18), which appears as orange-yellow in colour, equant with tabular crystals with pyramidal faces. Berry and Mason (1983) mentioned that wulfenite is a secondary mineral formed in the oxidized zone of ore deposits that contain lead and molybdenum-bearing minerals.

8-Galena (PbS) exists in the sample No. 2 (Fig. 13), it has a cubic structure or cube-octahedral morphology with a perfect cubic cleavage. Galena is lead-grey colour, and its major constituents are lead ore but silver, bismuth and thallium.

9-Natrolite (Na<sub>2</sub>Al<sub>2</sub>Si<sub>3</sub>O<sub>10</sub>•2H<sub>2</sub>O) is a common and popular zeolite mineral. It exists in the samples No. 2 and 3 (Fig. 19).

10-Jarosite KFe<sub>3</sub>+3(OH)<sub>6</sub>(SO<sub>4</sub>)<sub>2</sub> is brown to dark brown in colour and formed by the oxidation of iron sulfides. It was recorded in the samples No. 2, 3, and 4 (Figs. 19 and 22). Jarosite is often produced as a by-product during the purification and refining of zinc, as well as also commonly associated with acid mine drainage and acid sulfate soil environments.

11-Natro-Jarosite NaFe<sub>3</sub>+3(SO<sub>4</sub>)<sub>2</sub>(OH)<sub>6</sub> is brown in colour and it is closely related to the mineral jarosite, which recorded in the samples No. 4 and 9 (Fig. 20). Jarosite is iso-structural with natro-jarosite which means that they have the same crystal structure but different chemistries.

12-Titanite CaTiSiO<sub>5</sub> is yellowish brown in colour with elongated form and corroded edges. Titanite was recorded in the samples No. 4, 9 and 10, sometime; it variably contains other element such as iron, niobium, chromium, fluorine, sodium, manganese and yttrium (Figs. 20, 21 and 22). The crystal structure of Titanite can accommodate the REE available when the mineral

crystallized without appreciable fractionation.

13-Tychite Na<sub>6</sub>Mg<sub>2</sub>(CO<sub>3</sub>)<sub>4</sub>(SO<sub>4</sub>) is white in colour and it was recorded in the samples No. 6, 8, 9 and 10 (Fig. 18).

14-Anatase TiO<sub>2</sub> is reddish to yellowish brown in colour with double pyramids form. It was recorded in the samples No. 4, 9 and 10 (Fig. 20).

### **RADIOMETRIC INVESTIGATIONS**

Radiometric elements distributions in granitic rocks

Table (6) illustrates the concentration of the dose rate (D.R. nSvh-1), uranium (eU ppm), thorium (eTh ppm) and potassium (K%) of the studied granodiorite and syenogranite rocks, which they were measured in the field by portable RS-230 instrument.

The plot of eU vs. eTh diagram, illustrates that there is a positive correlation ( $r = 0.45$ ) in the studied granitic rocks, indicating their magmatic origin (Fig. 23). The calculated ratio of eTh/eU in the studied syenogranites is less than 3 indicating enrichment of uranium rather than thorium, where there is a negative correlation ( $r = -0.87$ ) between eU and eTh/eU in the all studied granitic rocks (Fig. 24).

Radiometric elements distribution in stream sediments

Table (7) and figure (25) illustrate the concentrated values for (D.R. nSvh-1), (eU ppm), (eTh ppm) and (K %) of the ten stream sediment pits. Each pit was measured two times; the first before taking the sample (surface) and the second after taking the sample (at depth).

- At pit No. 1, the measured values of D.R. is 285.5, eU is 18.60 and eTh is 28.50 at the surface, while they are 456.30, 45.60, and 23.50 respectively, at depth.

- At pit No.2, the measured values of D.R. is 467.6, eU is 18.60 and eTh is 92.0 at the surface, while they are 344.60, 16.0 and 51.60 respectively, at depth.

- At pit No.3, the measured values of D.R. is 168.30, eU is 5.70 and eTh is 21.40 at the surface, while they are 216.80, 10.80 and 29.90 respectively, at depth.

- At pit No.4, the measured values of D.R. is 188.70, eU is 11.10 and eTh is 16.20 at the surface, while they are 278.40, 13.50 and 29.20 respectively, at depth.

- At pit No.5, the measured values of D.R. is 286.0, eU is 15.80 and eTh is 37.90 at the surface, while they are 329.50, 16.60 and 51.70 respectively, at depth.

- At pit No.6, the measured values of D.R. is 169.9, eU is 6.50 and eTh is 19.90 at the surface, while they are 244.90, 9.60 and 26.50 respectively, at depth.

- At pit No.7, the measured values of D.R. is 134.30, eU is 5.50 and eTh is 13.20 at the surface, while they are 181.50, 8.60 and 16.90 respectively, at depth.

- At pit No.8, the measured values of D.R. is 158.60, eU is 5.50 and eTh is 17.60 at the sur-

face, while they are 217.7, 7.90 and 25.90 respectively, at depth.

- At pit No.9, the measured values of D.R. is 133.40, eU is 6.0 and eTh is 11.90 at the surface, while they are 134.7, eU is 6.60 and eTh is 9.50 respectively, at depth.

- At pit No.10, the measured values of D.R. is 152.0, eU is 5.0 and eTh is 16.60 at surface, while they are 191.70, eU is 7.50 and eTh is 21.80 respectively, at depth.

The above data, table (7) and figure (25) showing that the measured of the radioactive values increases with depth in the all pits except one No.2 at the studied stream sediments. The total average values of the D.R., K and eU are more than that in the granodiorites and less than that in the syenogranites.

Table 1: Chemical analysis of some trace elements for the granodiorites, syenogranites and stream sediments of the studied area at Southeast Wadi Ghadir.

Type of samples	S.No.	Cr	Ni	Cu	Zn	Zr	Rb	Y	Ba	Pb	Sr	Ga	V	Nb
Granodiorites	16	11	5	8	30	190	67	40	694	20	208	8	4	88
	17	9	6	7	20	202	77	30	798	16	355	9	5	87
	18	7	7	6	19	69	60	39	645	19	228	7	6	63
	19	9	6	7	11	219	75	41	860	18	363	6	7	79
	20	12	3	5	18	127	83	44	855	21	365	5	5	44
	Min.	7	3	5	11	69	60	30	645	16	208	5	4	44
	Max.	12	7	8	30	219	83	44	860	21	365	9	7	88
Aver.	9.6	5.4	6.6	19.6	161.4	72.4	38.8	770.4	18.8	303.8	7	5.4	72.2	
Syenogranites	11	24	14	9	50	179	277	80	271	17	6	13	5	32
	12	29	12	10	52	181	289	82	266	19	6	12	6	33
	13	26	13	9	47	180	258	79	265	16	7	11	6	32
	14	24	8	13	64	148	234	66	228	15	5	15	5	26
	15	25	15	12	54	175	265	77	258	18	8	14	7	29
	Min.	24	8	9	47	148	234	66	228	15	5	11	5	26
	Max.	29	15	13	64	181	289	82	271	19	8	15	7	33
Aver.	25.6	12.4	10.6	53.4	172.6	264.6	76.8	257.6	17	6.4	13	5.8	30	
Stream sediments	1	31	16	66	81	109	181	9	59	66	8	u.d	26	5
	2	35	20	88	100	166	226	13	69	70	13	u.d	31	7
	3	38	30	97	107	126	156	10	81	58	10	u.d	37	6
	4	33	21	81	98	130	190	11	71	62	11	u.d	35	7
	5	50	30	90	88	151	158	12	84	39	12	u.d	40	6
	6	34	18	80	66	89	170	7	48	40	7	u.d	22	4
	7	47	36	87	84	160	162	13	129	39	12	u.d	56	7
	8	42	24	81	79	132	156	10	83	33	11	u.d	37	6
	9	50	32	80	101	241	84	18	159	19	20	u.d	76	10
	10	50	22	76	113	141	187	11	75	53	12	u.d	37	6
	Min.	31	16	76	66	89	84	7	48	19	7	-	22	4
	Max.	50	36	97	113	241	226	18	159	70	20	-	76	10
Aver.	41	24.9	82.6	91.7	144.5	167	11.4	85.8	47.9	11.6	-	39.7	6.4	

Table 2: Correlation coefficient of the trace elements in the studied stream sediments, Southeast Wadi Ghadir.

Trace elements	Cr	Ni	Zn	Zr	Rb	Y	Ba	Sr	V
Nb	0.5	0.6	0.5	0.9		0.9	0.8	0.9	0.9
V	0.7	0.8		0.9		0.9	0.9	0.9	
Sr	0.6	0.5	0.5	0.9	0.6	0.9	0.8		
Pb					0.8				
Ba	0.7	0.8		0.9	0.7	0.9			
Y	0.6	0.6	0.5	0.9					
Rb									
Zr	0.6	0.6							
Cu		0.6							
Ni	0.7								

Table 3: Weight of heavy concentrates (1kg) after sieving and separation by bromoform with diagrammatic explanation attached, of the studied stream sediments samples, Southeast Wadi Ghadir.

S. No.	Weight of heavy concentrates (gram) after sieving of 1kg (>0.50mm)	Weight of heavy concentrates (gram) after sieving of 1kg (0.50-0.125mm)	Weight of heavy concentrates (gram) after sieving of 1kg (<0.125mm)	Weight of heavy concentrates (gram) after separation by bromoform (0.50-0.125mm)
1	905	50	45	2.8
2	901	48	51	2.6
3	905	55	40	3
4	896	58	46	4.6
5	888	52	60	3.2
6	920	45	35	1.4
7	909	48	43	1.6
8	892	57	51	3
9	898	60	42	5.6
10	896	56	48	2.6

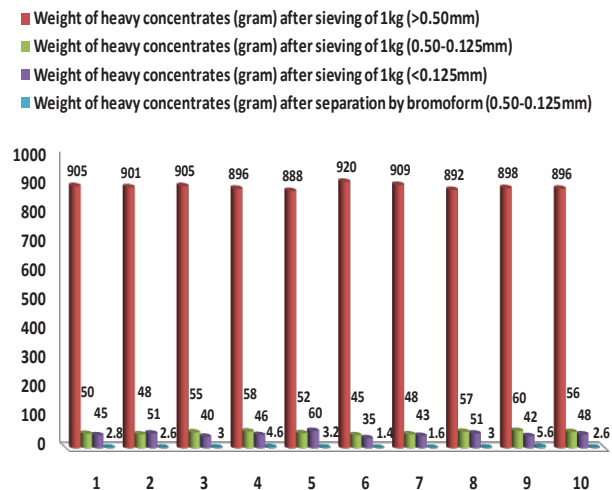
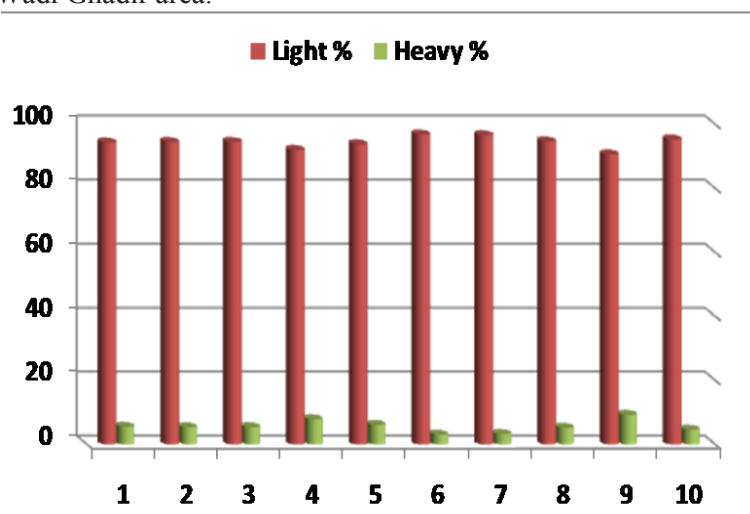


Table 4: Percentages of light and heavy minerals of the studied heavy concentrates (0.50-0.125mm), with histogram attached, Southeast Wadi Ghadir area.

S. No.	Light %	Heavy %
1	94.4	5.6
2	94.58	5.42
3	94.55	5.45
4	92.07	7.93
5	93.85	6.15
6	96.89	3.11
7	96.67	3.33
8	94.74	5.26
9	90.67	9.33
10	95.36	4.64



Sample No.	Identified minerals and/or mineral associations
1	Monazite, goethite, hematite and lepidocrocite,
2	Monazite, goethite, galena, jarosite and natrolite
3	Monazite, goethite, jarosite and natrolite
4	Goethite, jarosite, natro-jarosite, lepidocrocite, anatase and titanite
5	Goethite, hematite and lepidocrocite
6	Monazite, hematite, goethite and tychite
7	Hematite, goethite and monazite,
8	Monazite, hematite, goethite, pyrite and tychite
9	Goethite, cinnabar, hematite, tychite, natro-jarosite, anatase and titanite
10	Goethite, tychite, wulfenite, titanite, natro-jarosite and anatase

Table 6: Field radiometric measurements for the studied granodiorite and syenogranite rocks of Southeast Wadi Ghadir.

S. No.	Rock type	D.R. (nSvh <sup>-1</sup> )	K%	eU(ppm)	eTh(ppm)	eTh/eU
16	Granodiorites	190.1	4.1	5.6	22.6	4.04
17		175.1	4.8	4	22.6	5.65
18		169.7	4.9	4.2	19.6	4.67
19		160.6	4.1	5.7	23.6	4.14
20		143.4	3.5	6	24.9	4.15
Average		167.78	4.28	5.1	22.66	4.53
11	Syenogranites	209.1	4.3	10.4	27.3	2.63
12		223.8	4.8	10.9	23.5	2.16
13		424.2	5.5	38.8	25.2	0.65
14		364.6	5.8	29.1	25.2	0.87
15		267.4	5.9	13.6	25.9	1.90
Average		297.82	5.26	20.56	25.42	1.64

Table 7: Radiometric measurements on the studied stream sediments, Southeast Wadi Ghadir.

Sample No.	D.R.(nSvh-1)	K%	eU(ppm)	eTh(ppm)	Remarks
1	285.5	4.4	18.6	28.5	Surface
	456.3	5.1	45.6	23.5	After 30cm
2	487.6	4.1	18.6	92	Surface
	344.6	4.5	16	51.6	After 30cm
3	168.3	3.9	5.7	21.4	Surface
	216.8	4.9	10.8	29.9	After 30cm
4	188.7	4	11.1	16.2	Surface
	278.4	6	13.5	29.2	After 30cm
5	286	3.7	15.8	37.9	Surface
	329.5	4.1	16.6	51.7	After 30cm
6	169.9	3.9	6.5	19.9	Surface
	244.9	4.7	9.6	26.5	After 30cm
7	134.3	3.5	5.5	13.2	Surface
	181.5	4.4	8.6	16.9	After 30cm
8	158.6	4.1	5.5	17.6	Surface
	217.7	5.1	7.9	25.9	After 30cm
9	133.4	3.5	6	11.9	Surface
	134.7	3.8	6.6	9.5	After 30cm
10	152	4.1	5	16.6	Surface
	191.7	4.5	7.5	21.8	After 30cm
Average	216.43	3.92	9.83	27.52	Surface
Average	259.61	4.71	14.27	28.65	After 30cm
Total average	238.02	4.315	12.05	28.085	

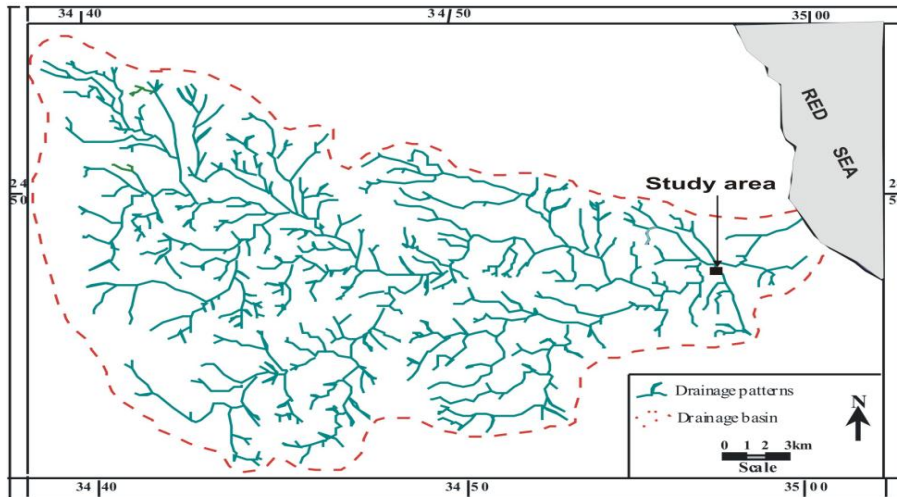


Fig. (1): Drainage map of Wadi Ghadir basin (Mahmoud, 2005)

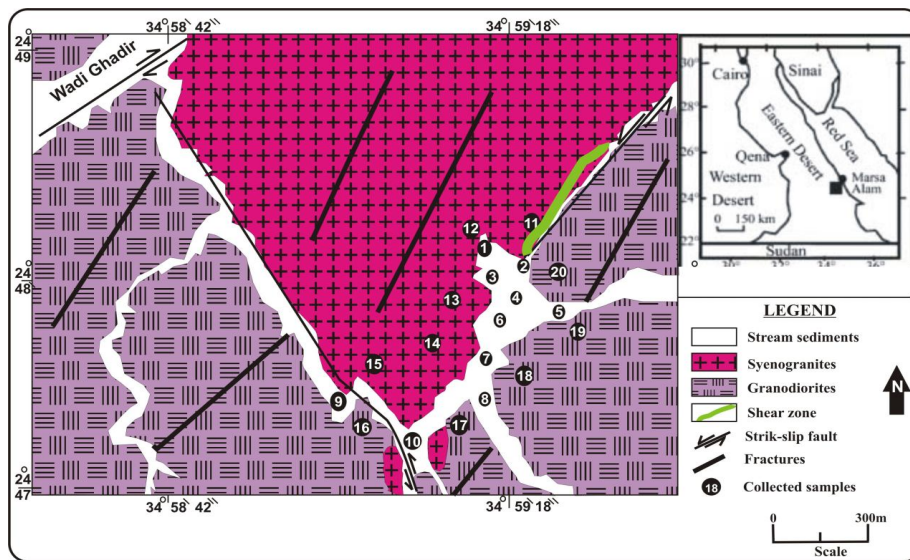


Fig. (2): Geological map of the studied Southeast Wadi Ghadir area, Southeastern Desert, Egypt (Modified after Takla et al., 1992 and Ibrahim and Ali, 2003).

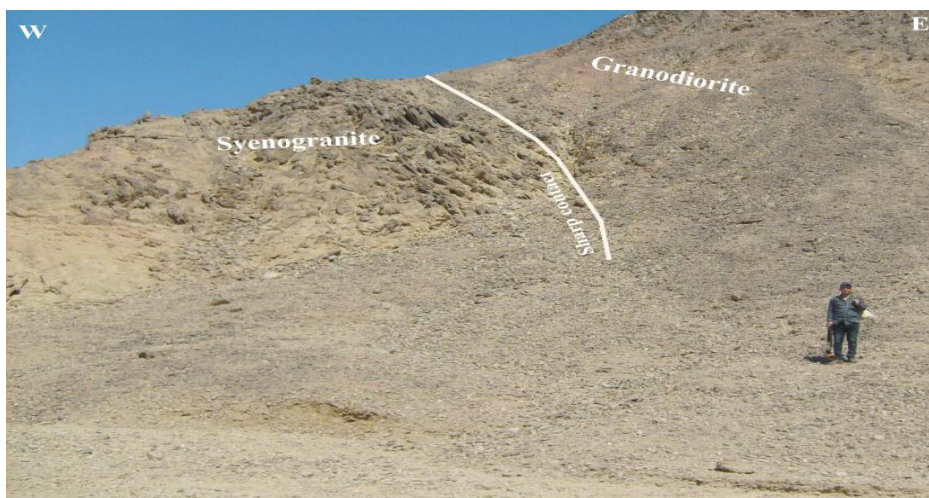


Fig. (3): Sharp contact between granodiorites and syenogranites at Southeast Wadi Ghadir area.

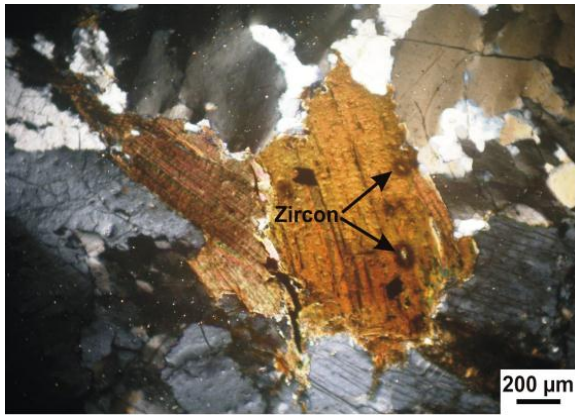


Fig. (4): Kaolinization and saussurization of K-feldspar and plagioclase, poikilitically enclosing quartz and opaque minerals in K-feldspar and biotite flakes corroded by undulose quartz in granodiorite rocks, Southeast Wadi Ghadir. Notice the crystals of zircon.

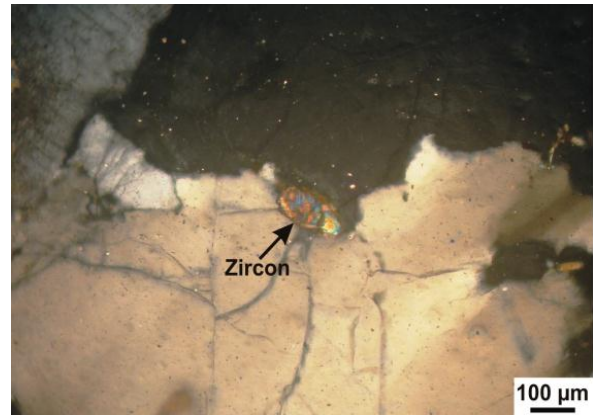


Fig. (5): Pleochroic haloes of zircon at the boundary between feldspar and quartz due to radiogenic effects, in granodiorite rocks, Southeast Wadi Ghadir. Notice some small crystals of titanite and apatite.

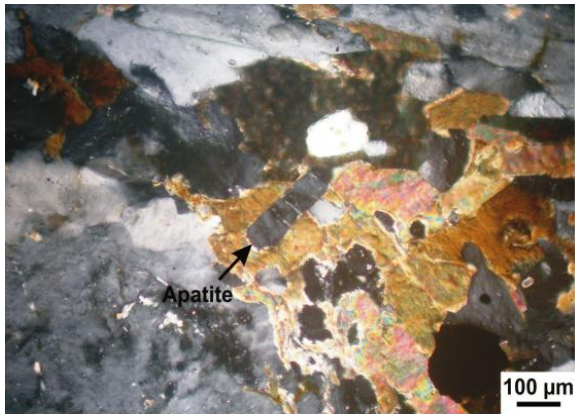


Fig. (6): Prismatic apatite associated with flakes of biotite and saussurite in plagioclase in syenogranite rocks, Southeast Wadi Ghadir.

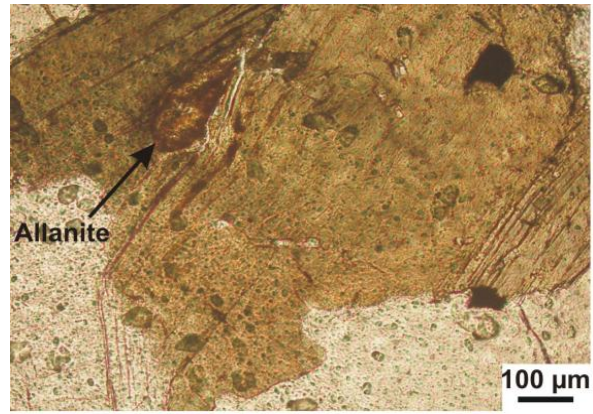


Fig. (7): Allanite associated with biotite in syenogranite rocks, Southeast Wadi Ghadir.



Fig. (8): Stream sediments pit with Rs-230 instrument at the studied area of Southeast Wadi Ghadir.

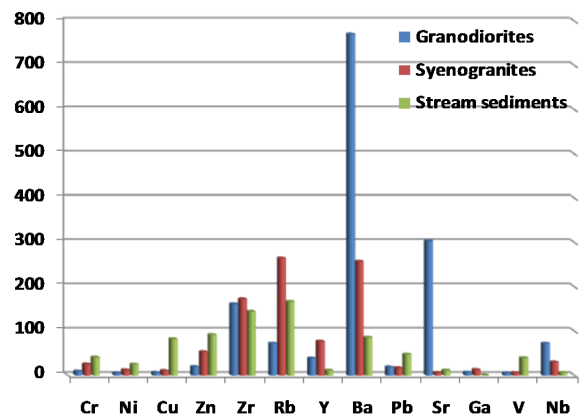


Fig. (9): Histogram showing the distribution of the trace elements in the granodiorites, syenogranites and stream sediments at the studied area, Southeast Wadi Ghadir.

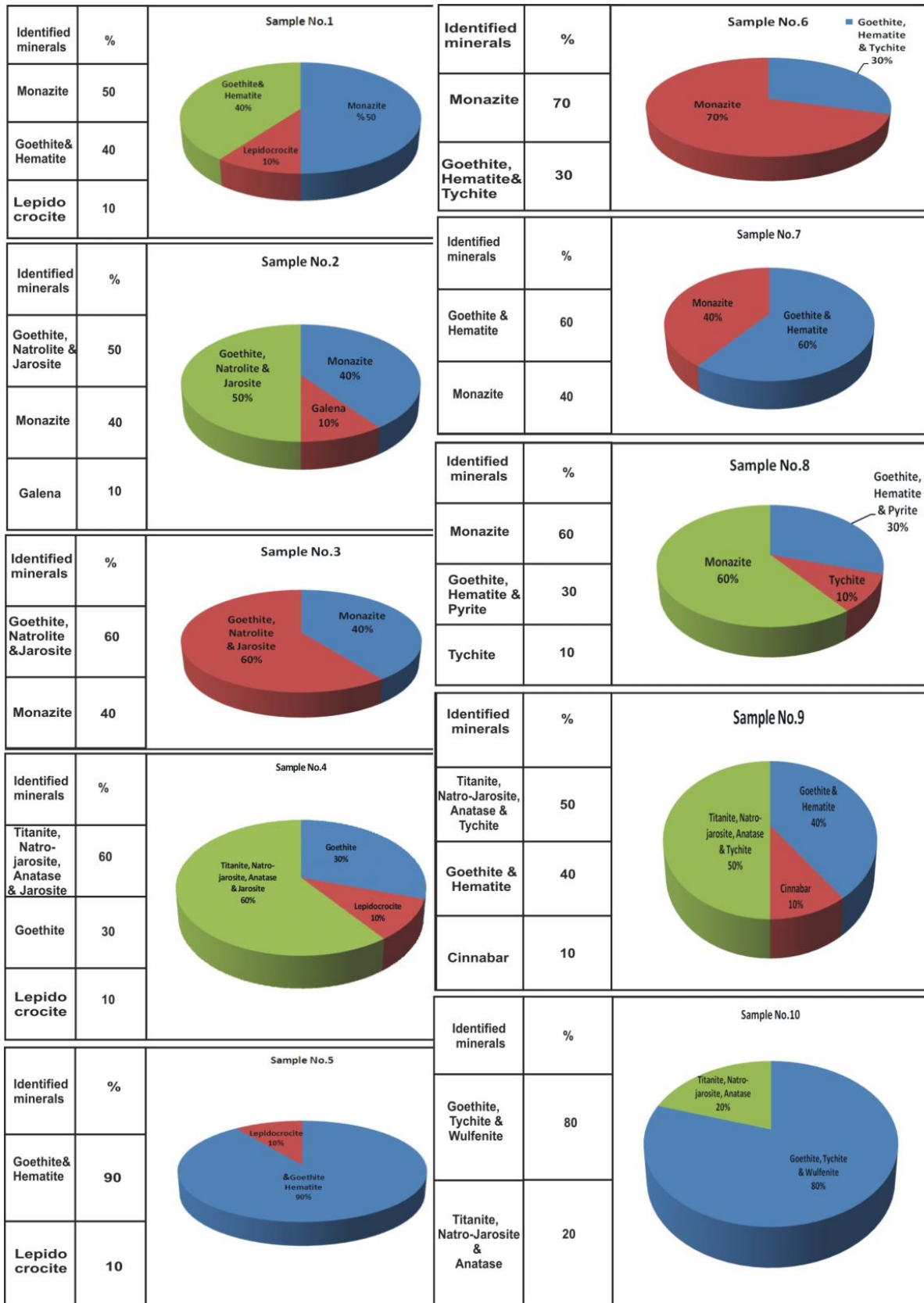
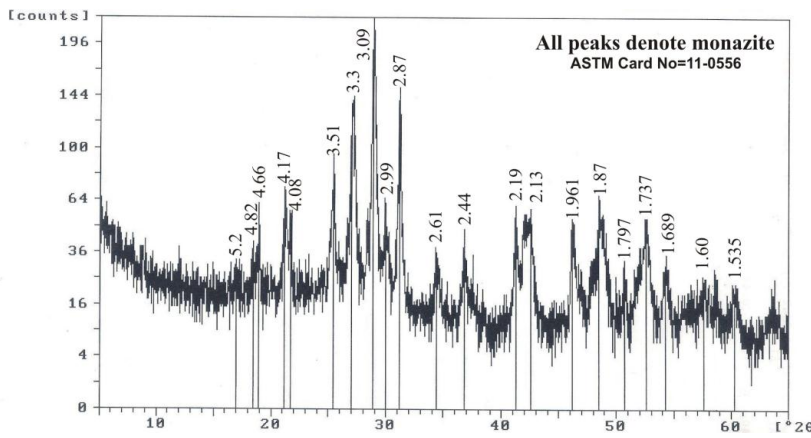


Fig. (10): Percentages of non-magnetic minerals in the studied stream sediment samples, Southeast Wadi Ghadir.

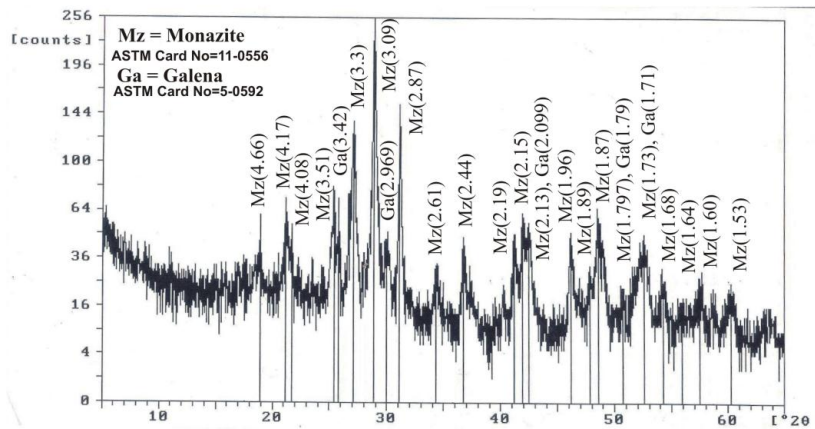


**Fig. (11):** Individual grains of some minerals species separated from the different studied stream sediment samples (A) Monazite, (B) lepidocrocite, (C) Goethite, (D) Hematite, (E) Pyrite and (F) Cinnabar.



**Fig. (12):** Shows the X-ray diffraction pattern of monazite from the studied stream sediments, Southeast Wadi Ghadir.

**Fig. (13):** Shows the X-ray diffraction pattern of monazite and galena from the studied stream sediments, Southeast Wadi Ghadir.



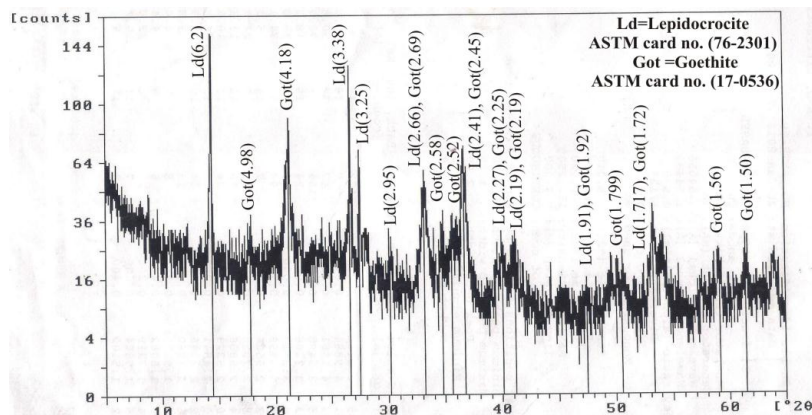


Fig. (14): Shows the X-ray diffraction pattern of Lepidocrocite and goethite from the studied stream sediments, Southeast Wadi Ghadir.

Fig. (15): Shows the X-ray diffraction pattern of hematite from the studied stream sediments, Southeast Wadi Ghadir.

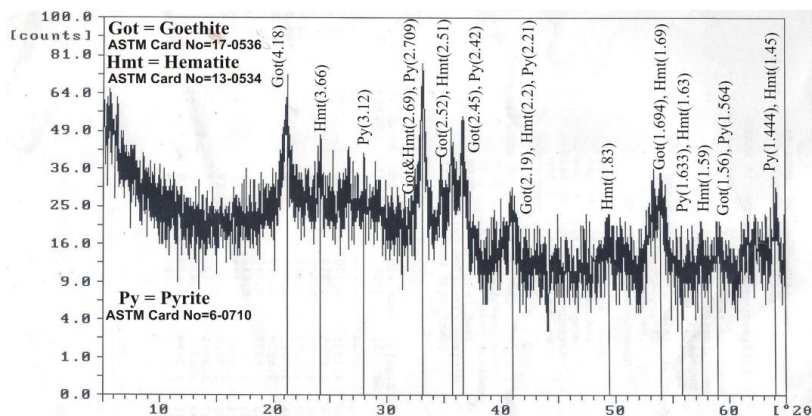
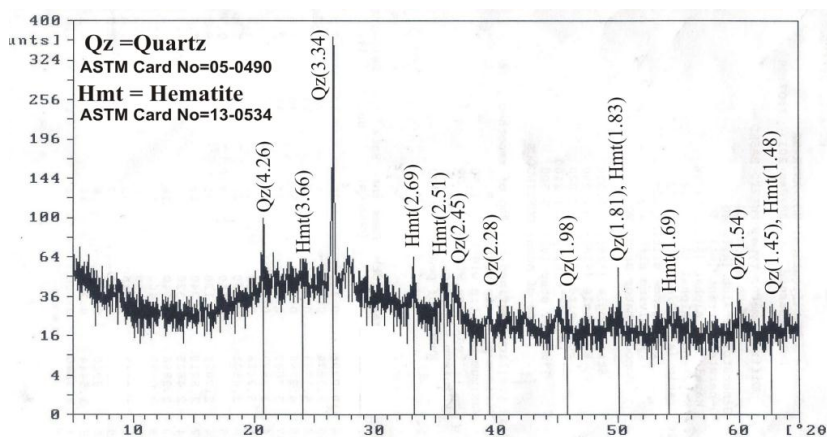
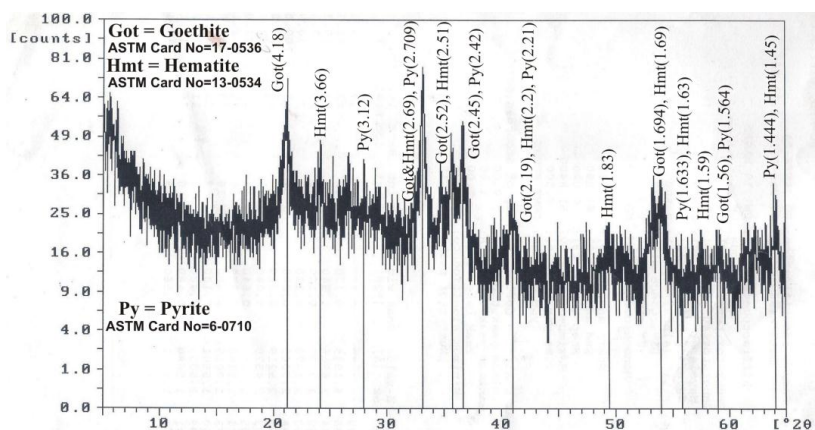


Fig. (16): Shows the X-ray diffraction pattern of goethite, hematite and pyrite from the studied stream sediments, Southeast Wadi Ghadir.

Fig. (17): Shows the X-ray diffraction pattern of cinnabar and epidote from the studied stream sediments, Southeast Wadi Ghadir.



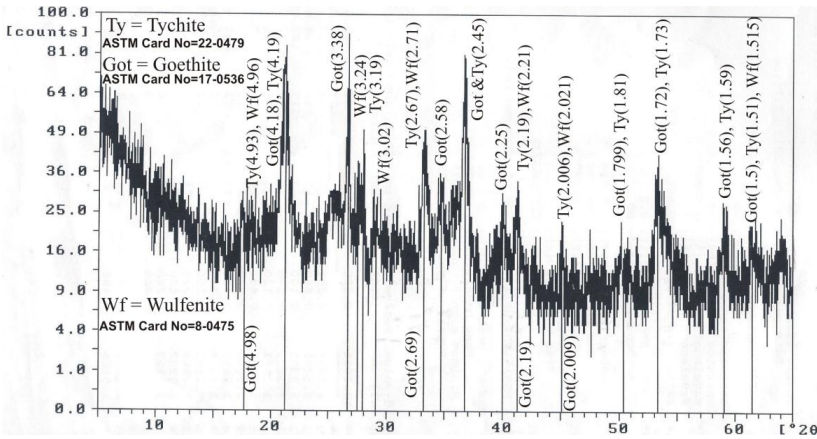


Fig. (18): Shows the X-ray diffraction pattern of ty-chite, goethite and wulfenite from the studied stream sediments, South-east Wadi Ghadir.

Fig. (19): Shows the X-ray diffraction pattern of natrolite, goethite and jarosite from the studied stream sediments, Southeast Wadi Ghadir.

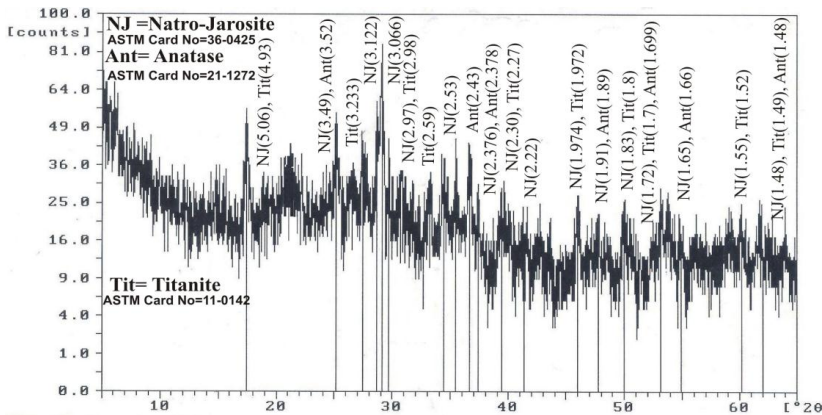
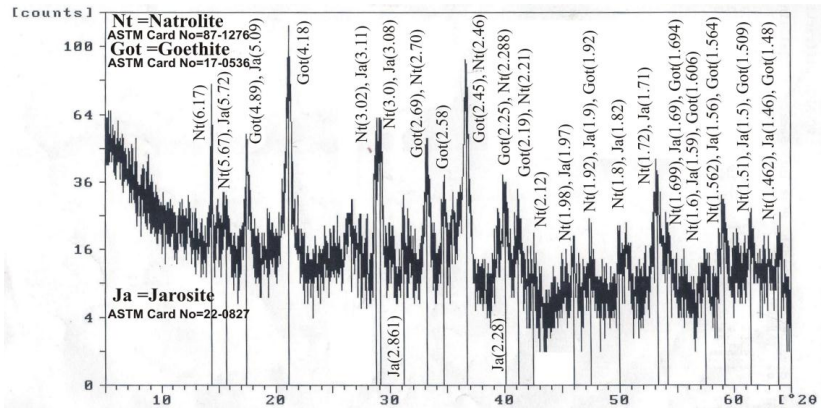
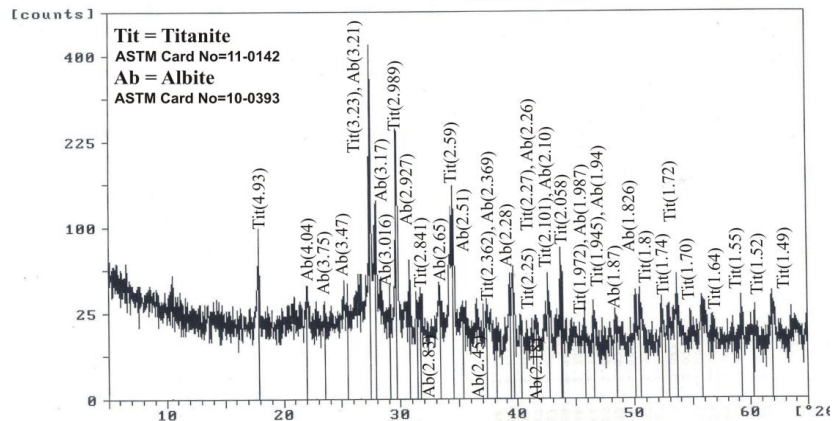


Fig. (20): Shows the X-ray diffraction pattern of natro-jarosite, anatase and titanite from the studied stream sediments, Southeast Wadi Ghadir.

Fig. (21): Shows the X-ray diffraction pattern of titanite from the studied stream sediments, South-east Wadi Ghadir.



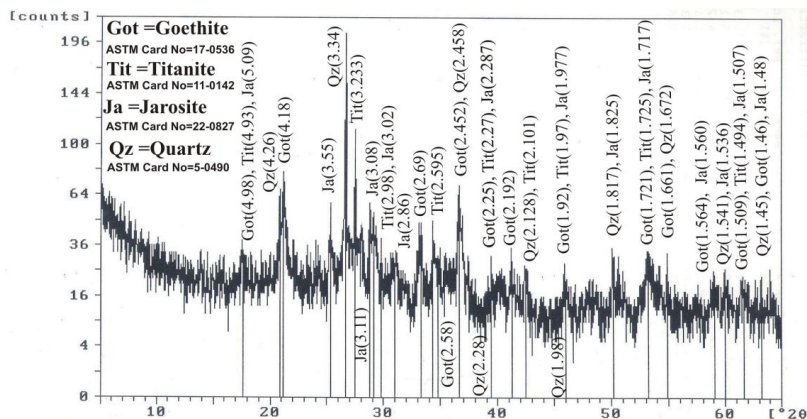


Fig. (22): Shows the X-ray diffraction pattern of goethite, titanite and jarosite from the studied stream sediments, Southeast Wadi Ghadir.

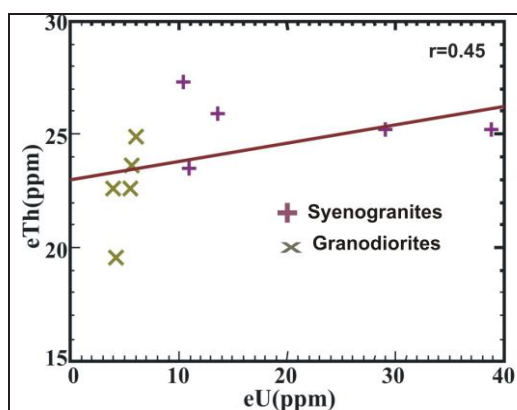


Fig. (23): Binary variation diagram showing the relation between eU vs. eTh of the studied granodiorite and syenogranite rocks, Southeast Wadi Ghadir.

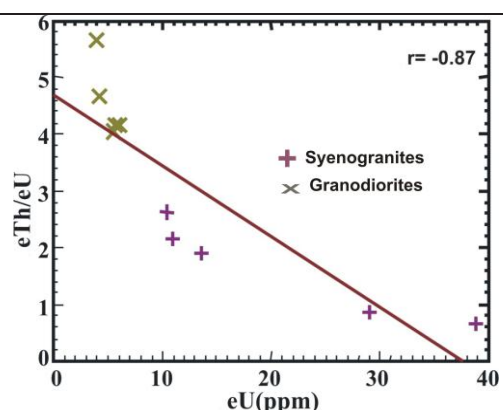


Fig. (24): Binary variation diagram showing the relation between eU vs. eTh/eU of the studied granodiorite and syenogranite rocks, Southeast Wadi Ghadir.

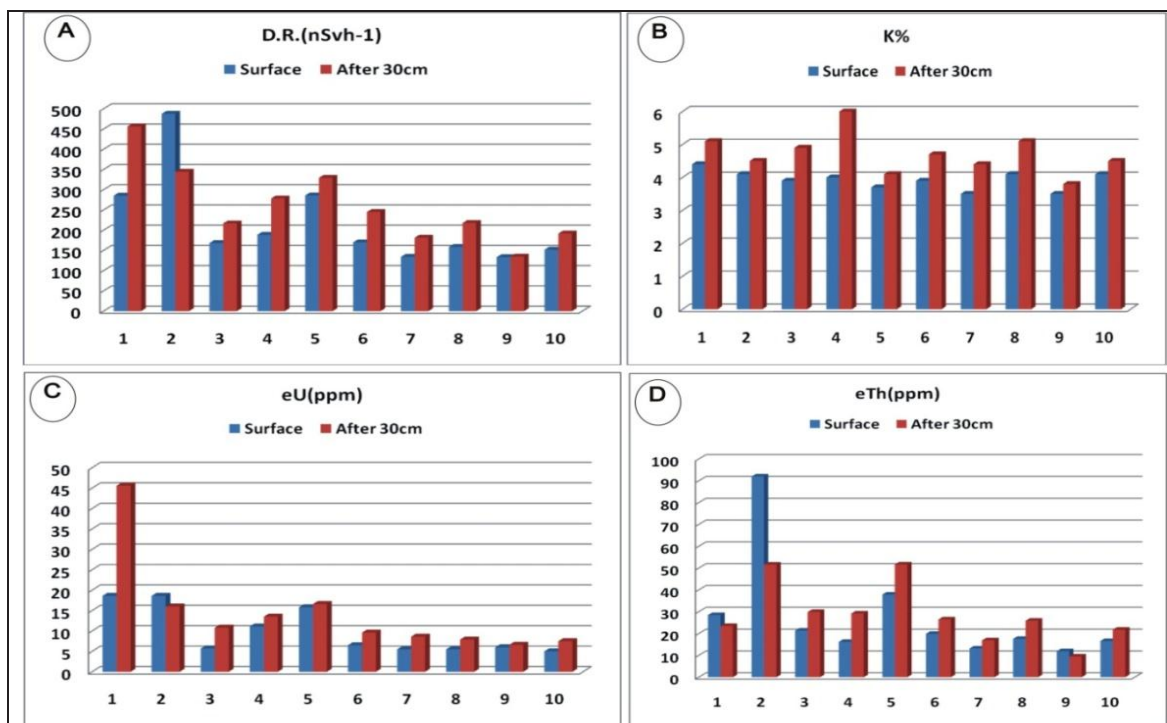


Fig. (25): Bar diagram for the radiometric measurements in studied stream sediments samples before and after taking the samples, at Wadi Ghadir area.

## CONCLUSION

Considering the geochemical analysis data of the studied stream sediments and its interpretation, can be deduced that the stream sediments of Southeast Wadi Ghadir area; originated from rocks highly enriched in trace minerals. Granodiorite and syenogranite rocks were recognized as a lithologic units in the studied area. Cr, Cu and Ni is the indicator elements for present the basic rocks (Ako 1980) surrounding the studied area. The geochemical data revealed that the studied stream sediments were originated from their surrounding rocks, this mean that the element distribution patterns and chemical composition of the studied stream sediments of Southeast Wadi Ghadir is greatly influenced by the local geology of the area. The correlation matrix reflects a very strong correlation between the all recorded trace elements (Table 2), indicating that they are governed by the same geochemical factors and are from the same source.

Estimation of heavy concentrates in the studied stream sediments starting with sample weight 1kg to be sieved into three parts; > 0.5mm, 0.50-0.125mm and < 0.125mm, and weighting for further treatments. The authors selected 0.5-0.125mm size fraction for study. The fraction was subjected to heavy minerals separation by using heavy liquid (bromoform, sp.gr. =2.85gm/cm<sup>3</sup>) to separate the heavy mineral fraction from the light mineral fractions. The heavy fractions were subjected to magnetic separation by using a Frantz isodynamic separator, which separate the heavy fraction into; magnetic and nonmagnetic minerals. The nonmagnetic minerals fractions are identified by using the X-ray diffraction technique. Some important minerals were recorded in this study such as; monazite, lepidocrocite, pyrite, cinnabar, wulfenite, galena and titanite. Finally, the percentage of the identified minerals at different stream sediments samples was estimated. The highest heavy mineral concentrates are recorded at sample no. 9, while sample no. 6 is the lowermost heavy mineral concentrates. Goethite, hematite and monazite are the most abundant minerals, while pyrite, galena and cinnabar are the lowest.

Radiometrically, the radioactivity increases towards the more acidic rocks from granodiorites to syenogranites. The syenogranites has eU more than twice Clark value; this indicates that the syenogranites were uraniferous. So, the studied syenogranites have been subjected to post-magmatic changes. Radiometric investigation of the studied stream sediments showed that the eU value (18.6 ppm) increase with the depth reached to eU value (45.6 ppm), indicating that uranium add to the stream sediments from the adjacent granitic rocks.

Finally, we are recommended that the studied area is weaked in Cu, Pb, Zn, and Ni concentrations merit further investigation to a certain if they can be pathfinders to gold mineralization in the studied area.

## ACKNOWLEDGMENT

The authors would like to express their wishes to thank Prof. Dr. Gehad M. Saleh for his help and reviewing the manuscript.

## REFERENCES

- Ahmed, N. A., 2001: Geomorphological and sedimentological studies on Pliocene-Quaternary alluvial fans, South Marsa Alam, Red Sea Egypt Ph.D thesis, faculty of science (Qena), South Valley University.
- Ako, B.D., 1980: A Contribution to Mineral Exploration in the Precambrian Belt of Part of South-western Nigeria. *J. Min. Geol.* 17 (2): 129-138.
- Ali, M. A., 2001: Geology, petrology and radioactivity of Gabal El-Sibai area, Central Eastern Desert, Egypt. Ph.D. Thesis, Cairo University, 300p.
- Ali, M.A., 2013: Mineral chemistry and genesis of Zr, Th, U, Nb, Pb, P, Ce and F enriched per-alkaline granites of El-Sibai shear zone, Central Eastern Desert, Egypt. *Geology*, Ju56/1, 107-128
- Ali, M. A. and Lentz, D.R., 2011: Mineralogy, Geochemistry and age dating of shear zone hosted Nb-Ta, Zr-Hf, Th-U bearing granitic rocks in the Ghadir and El-Sella areas, South Eastern Desert, Egypt. *Chin. J. Geochm.* vol.30, 453-478.
- Basta, E. Z., and Zaki, M., 1961: Geology and mineralization of Wadi Sikait area, south Eastern Desert, *J. geol. U.A. R.*, 5, No 1, 1-38.
- Berry, L. G. and Mason, B., 1983: Mineralogy: second ed., W. H. Freeman and Company, San Francisco, 561.
- Bowles, J. F. W., Jobbins, E. A. and Young, B. R., 1980: A re-examination of cheralite. *Mineral. Mag.*, 43, 885-888.

- El Bayoumi, R. M. A., 1980: Ophiolites and associated rocks of the Wadi Ghadir, east of Gebel Zabara. Eastern Desert, Egypt. Ph. D., thesis. Cairo Univ., Egypt, 227.
- El Gaby, S., 1975: Petrochemistry and geochemistry of some granites from Egypt. Neues Jrb. Mineral. Abh. 124, 147-189.
- El-Gaby, S. and Ahmed, A. A., 1980: The feiran – Solaf gneiss belt, SW Sinai, Egypt. – Inst. Appl. Geol., Jeddah, Bull. 3, 4, 95 – 105.
- El Gaby, S. and Habib, M. S., 1982: Geology of the area south west of Port Safaga with special emphasis on the granitic rocks. Eastern Desert, Egypt. Ann. Geol. Surv. Egypt. 12, 47-71.
- El Maghraby, A. M. O., 1987: the granitic rocks of Wadi Ghadir area, South Eastern Desert, Egypt. [M.Sc. thesis] Cairo Univ. Cairo, 300.
- El Nady, O. M., 1982: Geology of the Meatiq area. Central Eastern Desert, Egypt. Ph.D. thesis, Assuit Univ., Egypt.
- El Shazly, E. M. and Hassan, M. A., 1972: Geology and radioactive mineralization at Wadi Sikait- Wadi El Gemal area, south Eastern Desert, Egypt: Egypt. J. Geol. 16, no. 2, 201-234.
- El Shazly, E. M.; Hashad, A. H.; Sayyah, T. A. and Basyuni, F. A., 1973: Geochronology of Abu Swayel area, South Eastern Desert. Egyptian Jour. Geol., 17, 1-18.
- Habib, M. E., Ahmed, A. A., and El Nady, O.M., 1982: Lithostratigraphy and tectonic evolution of the Meatiq infrastructure. Central Eastern Desert, Egypt. In: Pan-African crustal evolution in Arabia and northeast Africa, Precambrian Res., v.16, (Abstract) p.A1-A58, Elsevier Sci. Publ. Co. Amsterdam. Handbook of physical contacts, Geol. Soc. Am. Mem. 97 sections
- Hassaan, M. M., 1974: Geochemical methods of prospecting for lead-zinc ore deposits in the Eastern Desert, Egypt. Ph.D. Dissertation, Leningard mining Institute, Leningard. (In Russian), 204.
- Hassaan, M. M. and Al-Hawary, M. A., 1989: Geochemical exploration in northern Eastern Desert II, mode of occurrence of copper and molybdenum in geochemical dispersion aureoles at Um Balad and Dara. Annals Geol. Surv. Egypt, XVI, 159-170.
- Hume, W. F., 1935: Geology of Egypt. V. II, Part II. The later Plutonic and intrusive rocks. Geol. Surv. Egypt. Government Press, Cairo, 301-688.
- Hussein, A. A., Ali, M. M. and El Ramly, M.F., 1982: A proposed new classification of the granites of Egypt. J. Volcan. And Geotherm. Res. 14, 187-198.
- Ibrahim, I.H. and Ali, M.A., 2003: The granitic rocks in Wadi Ghadir area, South Eastern Desert, Egypt and occurrence of a secondary uranium mineral [J]. Egyptian Journal of Geol. 47(2), 671–687.
- Jensen, L. S., 1976: A New Cation Plot for Classifying Sub-alkalic Volcanic Rocks, Ontario Division of Mines, MP 66, 22.
- Mahmoud, M. A. M., 2005: Geological studies of episyenite and related rocks as indications to uranium concentrations in Wadi Ghadir-Wadi El Gemal area, South Eastern Desert. M.Sc. thesis, Suez Canal Univ. Egypt, 145.
- Pabst, A. and Hutton, C. O., 1951: Huttonite, a new monoclinic thorium silicate. Am. Mineral., 36, 60-69.
- Raslan, M. F. and El-Feky, M. G., 2012: Radioactivity and mineralogy of the altered granites of the Wadi Ghadir shear zone, South Eastern Desert, Egypt. Chin. J. Geochem. 31:030–040
- Sabet, A. H., 1961: Geology and mineral deposits of Gabel El Sibai area, Red Sea Hills, Egypt. Ph. D. Thesis, Leiden State Univ. The Netherlands.
- Sabet, A. H., Tosogoev, V.B., Bessonenko, V.V., Baburin, I.M. and Pokryshkin, V.I., 1978: Some geological and tectonic peculiarities of the Central Eastern Desert of Egypt. Geol. Surv. Egypt, 6, 33-52.
- Saleh G. M., 1997: The potentiality of uranium occurrences in Wadi Nugrus area, south Eastern Desert, Egypt. Ph. D. Thesis Mans. Univ. 171.
- Schurmann, H. M. E., 1966: The Precambrian along the Gulf of Suez and the northern part of the Red Sea E. J. Brill, Leiden. 404.
- Shimron, A. E., 1980: Proterozoic island arc volcanism and sedimentation in Sinai. Precambrian Res., 12, 437-458.
- Takla, M. A., Basta, F. F. and El Maghraby, A. M. O., 1987a: Contribution to the geology of Wadi Ghadir area, South Eastern Desert, Egypt. 25th Ann. Meeting Geol. Soc. Egypt, Abstract, 17.
- Takla, M. A., Basta, F. F., and Surour, A. A., 1992: Petrology and mineral chemistry of rodingites associating the pan-African ultramafics of Sikait-Abu Rusheid area, south Eastern Desert, Egypt. Geology of the Arab world, Cairo Univ., 491-507.

معدنية وجيوكيميائية رواسب الوديان جنوب شرق وادى غدير - جنوب الصحراء الشرقية - مصر

محمود احمد محمد محمود، محمد سالم سالم قمر، حسين كمال الدين حسين

هيئة المواد النووية-القاهرة

يقع وادى غدير على بعد 30 كم جنوب غرب مدينة مرسى علم الساحلية بالبحر الأحمر حيث تقع منطقة الدراسة بين خطى الطول 34° 58' 18" و 34° 59' 30" وخطى العرض 24° 47' 00" و 24° 49' 00"

الغرض من هذه الدراسة هو معرفة تركيز العناصر الشحيحة والمعادن فى كل من رواسب الوديان والصخور المحيطة بها ثم عمل تقييم حسمى لهذه المعادن. تضم منطقة الدراسة نوعين من الصخور الجرانيتية، وهى صخور الجرانوديورايت و صخور السيانوجرانيت، حيث وجد ان تركيز بعض العناصر الشحيحة فى رواسب الوديان أعلى منها فى الصخور المحيطة. وتم التعرف على بعض المعادن المهمة مثل: المونازيت، البيريت، الهيماتيت، الجوتايت، الجالينا، الويلفنييت، السينابار، الجاروسيت والنتروجاروسيت. ووجد ان المونازيت والجوتايت والهيماتيت هى اكثر المعادن انتشارا وتركيزا بينما معادن البيريت والجالينا والسينابار هى الاقل تركيزا وانتشارا.

تم عمل القياسات الاشعاعية فى رواسب الوديان مرتين: الاولى قبل اخذ العينة ووجد ان اليورانيوم المكافئ يتراوح من 5 الى 19 جزء فى المليون والثوريوم المكافئ يتراوح من 11 الى 92 جزء فى المليون، والثانية بعد اخذ العينة على بعد 30 سم ووجد ان اليورانيوم المكافئ يتراوح من 6 الى 45.6 جزء فى المليون والثوريوم المكافئ يتراوح من 10 الى 52 جزء فى المليون حيث تزداد الاشعاعية مع العمق.